

Semiexclusive Processes: A different way to probe hadron structure¹

Carl E. Carlson

*Nuclear and Particle Theory Group, Physics Department,
College of William and Mary, Williamsburg, VA 23187-8795*

Abstract. Hard semiexclusive processes provide an opportunity to design effective currents to probe specific parton distributions and to probe in leading order parton distributions that fully inclusive reactions probe only via higher order corrections. High transverse momentum pion photoproduction is an example of a such a process. We discuss the perturbative and soft processes that contribute, and show how regions where perturbative processes dominate can give us the parton structure information. Polarized initial states are needed to get information on polarization distributions. Current polarization asymmetry data is mostly in the soft region. However, with somewhat higher energy, determining the polarized gluon distribution using hard pion photoproduction appears quite feasible.

SEMI-EXCLUSIVE PROCESSES AS PROBES OF HADRON STRUCTURE

This talk will discuss hard semiexclusive processes, namely processes of the form $B + A \rightarrow C + X$, where the momentum transfer $t = (p_B - p_C)^2$ is large [1–8]. Both the cases where the hadron C is part of a jet and where it is kinematically isolated are interesting. Semiexclusive processes provide the capability of designing “effective currents” [7] that probe specific parton distributions and for probing in leading order target distributions that are not probed at all in leading order in inclusive reactions.

Particle B can be a hadron or a real or virtual photon. We will here limit ourselves to the latter. The process we will discuss is

$$\gamma + A \rightarrow M + X, \quad (1)$$

where A is the target and M is a meson, for definiteness the pion. The process is perturbative because of the high transverse momentum of the pion, not because of the high Q^2 of the photon. Soft processes are from the present viewpoint an

¹⁾ Invited talk at the 12th Nuclear Physics Summer School and Symposium: New Directions in Quantum Chromodynamics, Kyongju, South Korea, 21–25 June 1999.

annoyance, but one we need to discuss and we will estimate their size farther below.

Our considerations also apply to electroproduction,

$$e + A \rightarrow M + X \quad (2)$$

when the final electron is not seen. We use the Weizäcker-Williams equivalent photon approximation [9] to relate the electron and photon cross sections,

$$d\sigma(eA \rightarrow MX) = \int dE_\gamma N(E_\gamma) d\sigma(\gamma A \rightarrow MX), \quad (3)$$

where the number distribution of photons accompanying the electron is a well known function.

In the following section, we will describe the subprocesses that contribute to hard pion production and show how the cross sections are dependent upon the parton densities and distribution amplitudes that we wish to probe, and in the subsequent section display some results. There will be a short summary at the end.

THE SUBPROCESSES

At the Highest k_T

At the highest possible transverse momenta, observed pions are directly produced at short range via a perturbative QCD (pQCD) calculable process [3–6]. Two out of four lowest order diagrams are shown Fig. 1. The pion produced this way is kinematically isolated rather than part of a jet, and may be seen either by making an isolated pion cut or by having some faith in the calculation and going to a kinematic region where this process dominates the others. Although this process is higher twist, at the highest transverse momenta its cross section falls less quickly than that of the competition, and we will show plots indicating the kinematics where it can be observed.

The subprocess cross section for direct or short-distance pion production is

$$\frac{d\hat{\sigma}}{dt}(\gamma q \rightarrow \pi^\pm q') = \frac{128\pi^2\alpha\alpha_s^2}{27(-t)\hat{s}^2} I_\pi^2 \left(\frac{e_q}{\hat{s}} + \frac{e'_q}{\hat{u}} \right) \left[\hat{s}^2 + \hat{u}^2 + \lambda h(\hat{s}^2 - \hat{u}^2) \right], \quad (4)$$

where \hat{s} , $\hat{t} = t$, and \hat{u} are the subprocess Mandelstam variables; λ and h are the helicities of the photon and target quark, respectively; and I_π is the integral

$$I_\pi = \int \frac{dy_1}{y_1} \phi_\pi(y_1, \mu^2). \quad (5)$$

In the last equation, ϕ_π is the distribution amplitude of the pion, and describes the quark-antiquark part of the pion as a parallel moving pair with momentum fractions y_i . It is normalized through the rate for $\pi^\pm \rightarrow \mu\nu$, and for example,

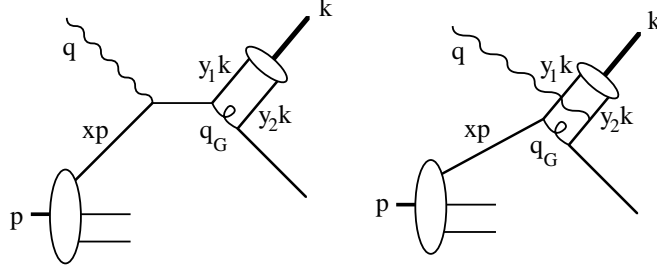


FIGURE 1. Direct pion production. The pion is produced in a short distance perturbatively calculated process, not by fragmentation of an outgoing parton. Thus this pion is kinematically isolated, and not part of a jet. Direct pion production gets important at very high transverse momentum because the pion does not have to share the available momentum with any other particles going in its direction.

$$\phi_\pi = \frac{f_\pi}{2\sqrt{3}} 6y_1(1 - y_1) \quad (6)$$

for the distribution amplitude called “asymptotic” and for $f_\pi \approx 93$ MeV. Overall,

$$\frac{d\sigma}{dx dt}(\gamma A \rightarrow \pi X) = \sum_q G_{q/A}(x, \mu^2) \frac{d\hat{\sigma}}{dt}(\gamma q \rightarrow \pi^\pm q'), \quad (7)$$

where $G_{q/A}(x, \mu^2)$ is the number distribution for quarks of flavor q in target A with momentum fraction x at renormalization scale μ .

There are a number of interesting features about direct pion production.

- For photoproduction, the struck quark’s momentum fraction is fixed by experimental observables. This is like deep inelastic scattering, where the experimenter can measure $x \equiv Q^2/2m_N\nu$ and this x is also the momentum fraction of the struck quark (for high Q and ν). For the present case, momenta are defined in Fig. 1 and the Mandelstam variables are

$$s = (p + q)^2; \quad t = (q - k)^2; \quad \text{and} \quad u = (p - k)^2. \quad (8)$$

The Mandelstam variables are all observables, and the ratio

$$x = \frac{-t}{s + u} \quad (9)$$

is the momentum fraction of the struck quark. We will let the reader prove this.

- The gluon involved in direct pion production is well off shell [3–5].
- Without polarization, we can measure I_π , given trust in the other parts of the calculation. This I_π is precisely the same as the I_π in both $\gamma^*\gamma \rightarrow \pi^0$ and $e\pi^\pm \rightarrow e\pi^\pm$.
- We have polarization sensitivity. For π^+ production at high x ,

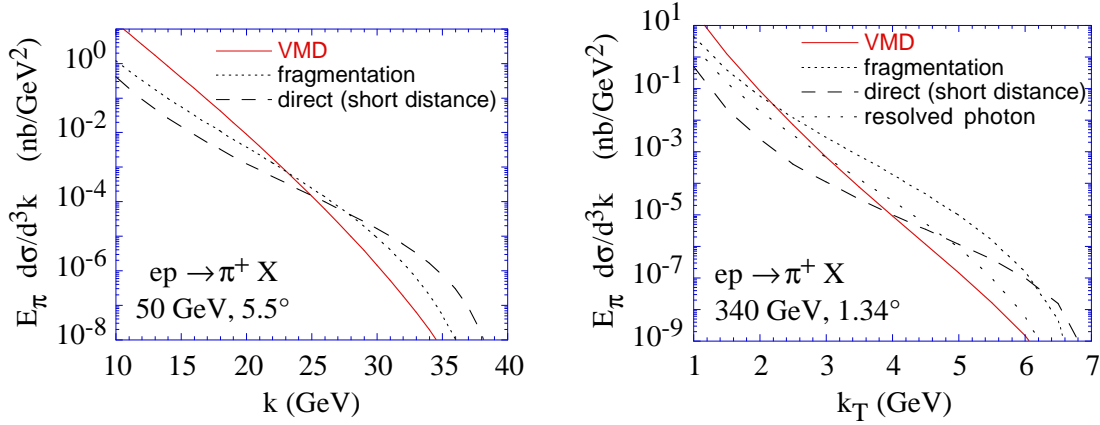


FIGURE 2. Calculated contributions to the cross section for $ep \rightarrow \pi^+ X$, with electron beam energies and pions emerging at angles in the target rest frame as indicated; k is the pion momentum. The 50 GeV plot shows a significant region where direct pion production dominates, once there is enough momentum that the soft (“VMD”) processes are not large. The 340 GeV plot shows a long window where the fragmentation process dominates.

$$A_{LL} \equiv \frac{\sigma_{R+} - \sigma_{L+}}{\sigma_{R+} + \sigma_{L+}} = \frac{s^2 - u^2}{s^2 + u^2} \cdot \frac{\Delta u(x)}{u(x)} \quad (10)$$

where R and L refer to the polarization of the photon, and $+$ refers to the target, say a proton, polarization. Also, inside a $+$ helicity proton the quarks could have either helicity, and

$$\Delta u(x) \equiv u_+(x) - u_-(x). \quad (11)$$

The large x behavior of both $d(x)/u(x)$ and $\Delta d(x)/\Delta u(x)$ are of current interest. Most fits to the data have the down quarks disappearing relative to the up quarks at high x , in contrast to pQCD which has definite non-zero predictions for both of the ratios in the previous sentence. Recent improved work on extracting neutron data from deuteron targets, has tended to support the pQCD predictions [10].

Experimentally, direct or short-range pion production can be seen. To show this, Fig. 2(left) plots the differential cross section for high transverse momentum π^+ electroproduction for a SLAC energy. Specifically, we have 50 GeV incoming electrons, with the pion emerging at 5.5° in the lab. It shows that above about 27 GeV total pion momentum or 2.6 GeV transverse momentum, direct (short distance, isolated) pion production exceeds its competition. Also shown in Fig. 2 is a situation where there is a long region where the fragmentation process—next up for discussion—dominates. Incidentally, the 340 GeV energy for the electron beam on stationary protons was chosen to match recent very preliminary discussions of an Electron Polarized Ion Collider (EPIC) with 4 GeV electrons and 40 GeV protons, and the 1.34° angle in the target rest frame matches 90° in the lab for such a collider.

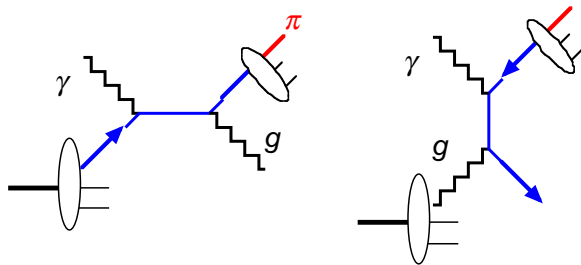


FIGURE 3. The fragmentation process. Pions are produced by fragmentation of partons at long distances from the primary interaction region. The Compton process is on the left; the pion could come from either quark or gluon fragmentation. Quark-gluon fusion is on the right.

Moderate k_T

At moderate transverse momentum, the generally dominant process is still a direct interaction in the sense that the photon interacts directly with constituents of the target, but the pion is not produced directly at short range but rather at long distances by fragmentation of some parton [1,2,5]. Many authors refer to this as the direct process; others of us are in the habit of calling it the fragmentation process. The main subprocesses are called the Compton process and photon-gluon fusion, and one example of each is shown in Fig. 3.

Photon gluon fusion often gives 30–50% of the cross section for the fragmentation process, and the polarization asymmetry is as large as can be in magnitude,

$$\hat{A}_{LL}(\gamma g \rightarrow q\bar{q}) = -100\%. \quad (12)$$

Typically for the Compton process, $\hat{A}_{LL}(\gamma q \rightarrow gq) \approx 1/2$. We shall show some A_{LL} plots for the overall process after we discuss the soft processes.

We should note that the NLO calculations for the fragmentation process have been done also for the polarized case, though our plots are based on LO. For direct pion production, NLO calculations are not presently completed.

We should also remark that the photon may split into hadronic matter before interacting with the target. If splits into a quark anti-quark pair that are close together, the splitting can be modeled perturbatively or quasi-perturbatively, and we call it a “resolved photon process.” A typical diagram is shown in the left hand part of Fig. 4. Resolved photon processes are crucial at HERA energies, but not at energies under discussion here, and we say no more about them.

Soft Processes

This is the totally non-perturbative part of the calculation, whose size can be estimated by connecting it to hadronic cross sections. The photon may turn into hadronic matter, such as $\gamma \rightarrow q\bar{q} + \dots$ with a wide spatial separation. It can be represented as photons turning into vector mesons. See Fig. 4(right).

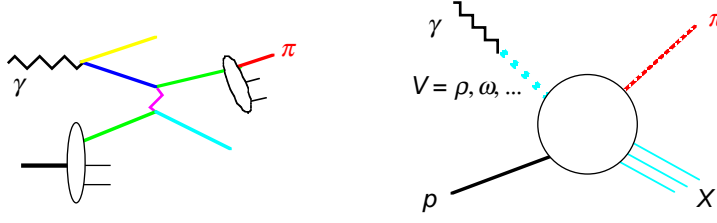


FIGURE 4. Resolved photon process (left) and vector meson dominated process (right).

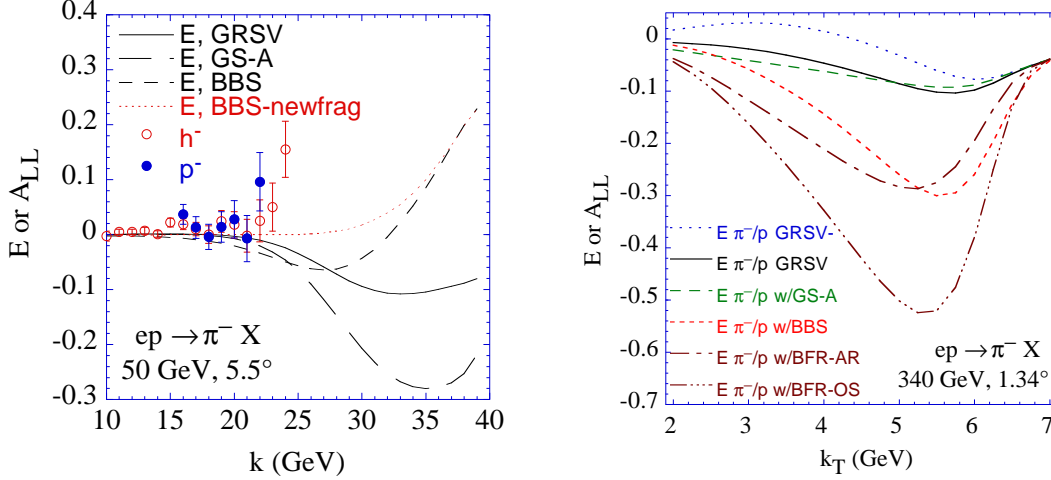


FIGURE 5. Longitudinal polarization asymmetries for π^- production for two energies and target rest frame angles as labeled. A description of the curves is given in the text.

We want a reliable approximation to the non-perturbative cross section so we can say where perturbative contributions dominate and where they do not. To get such an approximation one can start with the cross section given as

$$d\sigma(\gamma A \rightarrow \pi X) = \sum_V \frac{\alpha}{\alpha_V} d\sigma(V + A \rightarrow \pi X) + (\text{non-VMD}), \quad (13)$$

where the sum is over vector mesons V , $\alpha = e^2/4\pi$, and $\alpha_V = f_V^2/4\pi$. We can get, for example, f_ρ from the decay $\rho \rightarrow e^+e^-$. Then “all” one needs is a parameterization of the hadronic process, based on data. Details of our implementation of this program are given in [12].

We took the soft processes to be polarization insensitive. This agrees with a recent Regge analysis of Manayenkov [13].

RESULTS

Since results for the unpolarized cross section have already been displayed in Fig. 2, we focus on results for A_{LL} , which is also called E by some authors [14]. Fig. 5 shows two plots, both for π^- production.

The 50 GeV plot, Fig. 5(left), is dominated by direct pion production above the soft region, and is sensitive mainly to the differing polarized quark distributions of the different models. Three different parton distribution models are shown [17–19]. Although the fragmentation process is not the crucial one here, we should mention that mostly we used our own fragmentation functions [3], and that the results using a better known set [15] are not very different. Neither set of fragmentation functions agrees well with the most recent HERMES data [16] for unfavored vs. favored fragmentation functions, and the one curve labeled “newfrag” is calculated with fragmentation functions that agree better with that data.

Below about 20 GeV total pion momentum where the soft process dominates, the data is well described by supposing the soft processes are polarization independent. Above that, with asymmetry due to perturbative processes, the difference among the results for the different sets of parton distributions is quite large for the π^- .

The data is from Anthony *et al.* [11]. Presently most of the data is in the region where the soft processes dominate. The data is already interesting. Further data at even higher pion momenta would be even more interesting. Regarding the differences among the quark distributions, recall that large momentum corresponds to $x \rightarrow 1$ for the struck quark, and pQCD predicts that the quarks are 100% polarized in this limit. Only the parton distributions labeled BBS [17] are in tune with the pQCD prediction, and they for large momentum predict even a different sign for A_{LL} for the π^- . Calculated results plotted with the data for the π^+ and for deuteron targets may be examined in [12].

The other plot in Fig. 5 is for 340 GeV electron beam energy, an energy where there is a long region where the fragmentation process dominates. We would like to know how sensitive the possible measurements of A_{LL} are to the different models for Δg . To find out, Fig. 5 (right) presents calculated results for A_{LL} for one set of quark distributions and 5 different distributions for Δg [17–20]. The quark distributions and unpolarized gluon distribution in each case are those of GRSV [18]. There are 6 curves on each figure. One of them (labeled GRSV–) is a benchmark, which was calculated with Δg set to zero. The other curves use the Δg from the indicated distribution. There is a fair spread in the results, especially for the π^- where photon-gluon fusion gives a larger fraction of the cross section. Thus, one could adjudicate among the polarized gluon distribution models.

SUMMARY

Several perturbative processes contribute to hard pion photoproduction. All are calculable. They give us new ways to measure aspects of the pion wave function, and quark and gluon distributions, especially Δq and Δg . The soft processes can be estimated and avoided if the transverse momentum is greater than about 2 GeV. SLAC or HERMES energies would be excellent for finding direct pion production, which is sensitive to Δu and Δd , and higher energies would give a region where the fragmentation process dominates and be excellent for measuring Δg .

ACKNOWLEDGMENTS

My work on this subject has been done with Andrei Afanasev, Chris Wahlquist, and A. B. Wakely and I thank them for pleasant collaborations. I have also benefited from talking to and reading the work of many authors and apologize to those I have not explicitly cited. I thank the NSF for support under grant PHY-9900657.

REFERENCES

1. De Florian, D., and Vogelsang, W., *Phys. Rev. D* **57**, 4376 (1998); Kniehl, B. A., Talk at Ringberg Workshop, hep-ph/9709261; Stratmann, M., and Vogelsang, W., Talk at Ringberg Workshop, hep-ph/9708243.
2. Peralta, J. J., Contogouris, A. P., Kamal, B., and Lebessis, F., *Phys. Rev. D* **49**, 3148 (1994).
3. Carlson, C. E., and Wakely, A. B., *Phys. Rev. D* **48**, 2000 (1993).
4. Afanasev, A., Carlson, C. E., and Wahlquist, C., *Phys. Lett. B* **398**, 393 (1997).
5. Afanasev, A., Carlson, C. E., and Wahlquist, C., *Phys. Rev. D* **58**, 054007 (1998).
6. Brodsky, S. J., Diehl, M., Hoyer, P., and Peigne, S., *Phys. Lett. B* **449**, 306 (1999).
7. Brodsky, S. J., Talk presented at the EPIC'99 Workshop, Indiana University Cyclotron Facility, Bloomington, Indiana, April 8–11, 1999, hep-ph/9907346.
8. Carlson, C. E., Talk presented at the EPIC'99 Workshop, Indiana University Cyclotron Facility, Bloomington, Indiana, April 8–11, 1999, hep-ph/9905492.
9. See for example the Appendix to Brodsky, S. J., Kinoshita, T., and Terazawa, H., *Phys. Rev. D* **4**, 1532 (1971).
10. Melnitchouk, W., Speth, J., and Thomas, A. W., *PLB* **435**, 420 (1998); Melnitchouk, W., and Peng, J.C., *Phys. Lett. B* **400**, 220 (1997); Melnitchouk, W., and Thomas, A. W., *Phys. Lett. B* **377**, 11 (1996); Yang, U. K., and Bodek, A., *Phys. Rev. Lett.* **82**, 2467 (1999).
11. Anthony, P. L. *et al.*, *Phys. Lett. B* **458**, 536 (1999).
12. Afanasev, A., Carlson, C. E., and Wahlquist, C., hep-th/9903493.
13. Manayenkov, S. I., report DESY 99-016, hep-ph/9903405.
14. Barker, I. S., Donnachie, A., and Storrow, J. K., *Nucl. Phys. B* **95**, 347 (1975).
15. Binneweis, J., Kniehl, B. A., and Kramer, G., *Z. Phys. C* **65**, 471 (1995) and *Phys. Rev. D* **52**, 4947 (1995).
16. Makins, N., Proceedings of CEBAF Workshop on Physics and Instrumentation with 6-12 GeV Beams, ed. S. Dytman, H. Fenker, and P. Roos, JLab, Newport News, June 1998, p.97; Geiger, Ph., *Measurement of Fragmentation Functions at HERMES*, Ph. D. Thesis, Ruprecht-Karls-Universität, Heidelberg, 1998.
17. Brodsky, S. J., Burkardt, M., and Schmidt, I., *Nucl. Phys. B* **441**, 197 (1995).
18. Glück, M., Reya, E., Stratmann, M., and W. Vogelsang, *Phys. Rev. D* **53**, 4775 (1996).
19. Gehrmann, T., and Stirling, W. J., *Phys. Rev. D* **53**, 6100 (1996).
20. Ball, R. D., Forte, S., and Ridolfi, G., *Phys. Lett. B* **378**, 255 (1996).